



# Cancer Research

## An Anti-ICAM-2 (CD102) Monoclonal Antibody Induces Immune-mediated Regressions of Transplanted ICAM-2-negative Colon Carcinomas

Ignacio Melero, Izaskun Gabari, Angel L. Corbí, et al.

*Cancer Res* 2002;62:3167-3174.

**Updated Version** Access the most recent version of this article at:  
<http://cancerres.aacrjournals.org/content/62/11/3167>

**Cited Articles** This article cites 39 articles, 16 of which you can access for free at:  
<http://cancerres.aacrjournals.org/content/62/11/3167.full.html#ref-list-1>

**Citing Articles** This article has been cited by 6 HighWire-hosted articles. Access the articles at:  
<http://cancerres.aacrjournals.org/content/62/11/3167.full.html#related-urls>

**E-mail alerts** [Sign up to receive free email-alerts](#) related to this article or journal.

**Reprints and Subscriptions** To order reprints of this article or to subscribe to the journal, contact the AACR Publications Department at [pubs@aacr.org](mailto:pubs@aacr.org).

**Permissions** To request permission to re-use all or part of this article, contact the AACR Publications Department at [permissions@aacr.org](mailto:permissions@aacr.org).

# An Anti-ICAM-2 (CD102) Monoclonal Antibody Induces Immune-mediated Regressions of Transplanted ICAM-2-negative Colon Carcinomas<sup>1</sup>

Ignacio Melero,<sup>2</sup> Izaskun Gabari, Angel L. Corbí, Miguel Relloso, Guillermo Mazzolini, Volker Schmitz, Mercedes Rodriguez-Calvillo, Iñigo Tirapu, Emilio Camafeita, Juan P. Albar, and Jesús Prieto

Gene Therapy Unit, Department of Medicine, University of Navarra School of Medicine, 31008 Pamplona [I. M., I. G., G. M., V. S., M. R.-C., I. T., J. P.]; Proteomics Facility and Department of Immunology and Oncology, Centro Nacional de Biotecnología (Farmacia/ Consejo Superior de Investigaciones Científicas), Canto Blanco, E-28049 Madrid [E. C., J. P. A.]; and Centro de Investigaciones Biológicas, Consejo Superior de Investigaciones Científicas, 28006 Madrid [A. L. C., M. R.] Spain

## ABSTRACT

Monoclonal antibodies (mAbs) can mediate antitumor effects by indirect mechanisms involving antiangiogenesis and up-regulation of the cellular immune response rather than by direct tumor cell destruction. From mAbs raised by immunization of rats with transformed murine endothelial cells, a mAb (EOL4G8) was selected for its ability to eradicate a fraction of established colon carcinomas that did not express the EOL4G8-recognized antigen. The antigen was found to be ICAM-2 (CD102). Antitumor effects of EOL4G8, which required a functional T-cell compartment, were abrogated by depletion of CD8<sup>+</sup> cells and correlated with antitumor CTL activity, whereas only a mild inhibition of angiogenesis was observed. Interestingly, we found that EOL4G8 acting on endothelial ICAM-2 markedly enhances leukotactic factor activity-1-independent adhesion of immature dendritic cells to endothelium—an effect that is at least in part mediated by DC-SIGN (CD209).

## INTRODUCTION

mAbs<sup>3</sup> have been used to inflict selective damage to malignant cells *in vivo* both in animal experimentation and at the clinic (1). More recently, mAbs have been used to elicit indirect mechanisms that efficiently treat tumors by potentiating the immune response (2–4) or by decreasing angiogenesis in the malignant tissue (5, 6).

To identify novel antibody specificities that could operate through these indirect mechanisms, we immunized rats with mouse endothelioma cells and searched for mAbs displaying antitumor effects *in vivo*. We found one antibody fulfilling such features that recognized the adhesion molecule ICAM-2 (CD102). This surface antigen is a glycoprotein that belongs to the Ig superfamily encompassing two Ig domains (7–9). It was functionally identified in humans as a counter-receptor for the leukocyte integrin LFA-1 (8). Tissue distribution for ICAM-2 in humans includes constitutive expression on endothelial cells as well as on T and B lymphocytes (7). Recently a second counter-receptor for ICAM-2 has been identified selectively expressed on human DCs, and that molecule is the C-type lectin named DC-SIGN (CD209; Refs. 10–13). DC-SIGN was originally described as a selective ligand for ICAM-3 (12), but recently its binding to ICAM-2 was found to be stronger, and it has been shown to be involved in the traffic of DCs to tissues (10). Mannose-containing

moieties attached on ICAMs are involved in the binding to DC-SIGN (14). Besides its proposed role in cell traffic, DC-SIGN is important at the immunological synapse that is formed by T cells and antigen-presenting DCs (13, 15). A number of DC-SIGN murine homologues have been identified recently, but information on its function is not available yet, although one of the homologues is expressed in DCs at the RNA level (16). ICAM-2<sup>-/-</sup> mice develop normal immune responses and accordingly the function of this molecule is largely dispensable (17), indicating that its function is probably redundant with other proteins of its family.

This study demonstrates that *in vivo* treatment with anti-ICAM-2 mAb can cure established transplanted colon carcinomas that are completely ICAM-2-negative through mechanisms that are dependent on the induction of tumor-specific CTL-mediated immune responses. Evidence has been obtained that ICAM-2 bound by EOL4G8 up-regulates its adhesiveness to DC-SIGN, providing a mechanistic rationale to the enhancement of antitumor immunity.

## MATERIALS AND METHODS

**Cell Lines, Antibodies, and Reagents.** MC38 and CT26 have been described previously (18). PY-4.1 and H5V are SV40 T-transformed endotheliomas (19, 20) generously given by V. Bautch (University of North Carolina, Chapel Hill, NC) and A. Mantovani (Istituto Mario Negri, Milan, Italy). These cells have been derived from transgenic mice ubiquitously expressing SV40 T antigen. D2SC/1 is a spleen-derived murine DC line (kindly provided by P. Ricciardi-Castagnoli, University of Milan, Italy; Refs. 21, 22). Human DC-SIGN-expressing transfectants in K562 cells and the anti DC-SIGN mAb (MR-1) have been described (23). 3C8 antimouse ICAM-2 was from PharMingen (Heidelberg, Germany) as well as anti-ICAM-1, anti-VCAM-1, anti H-2L<sup>d</sup>, anti H-2K<sup>b</sup>, anti-CD3 anti-CD28, anti-LFA-1, anti-CD31, and secondary FITC-tagged antirat IgG and IgG2b antibodies. Hybridoma production and purification of EOL4G8 mAb was as described (24). The screening was performed by selecting out antibodies binding PY4–1 but not various carcinoma cell lines. Hybridomas fulfilling both criteria were grown as ascites in BALB/c-*nu/nu* mice, and ascites fluid was tested for *in vivo* interference of CT26-derived tumors implanted in syngeneic mice by giving it inside tumor nodules. Anti-CD8-depleting antibody was ascitic fluid of the hybridoma H35–17.2 (American Type Culture Collection; Ref. 25). TS2.18 antihuman CD18 was from Francisco Sanchez-Madrid (Hospital de la Princesa, Spain). Antibody-conjugated magnetic beads and cell separation protocols were from Miltenyi (Bergisch Gladbach, Germany). Rat IgG, Colchicine, ConA, and EGTA were from Sigma (Madrid, Spain). Culture medium and FCS were from Life Technologies, Inc. (Cergy-Pontoise, France).

**Flow Cytometry and Immunohistochemistry.** Indirect and direct immunofluorescence and flow cytometry were performed as described (24) using a FACS-Scalibur (Becton Dickinson, Mountain View, CA). Cryosections were prepared and processed for indirect immunohistochemical staining as described (24).

**Immunoprecipitation and Western Blot.** PY4.1 cells were surface biotinylated with sulfo-NHS-Biotin (Pierce, Rockford, IL), lysed, and immunoprecipitates were obtained as described (24, 26). Immunoprecipitates were analyzed by SDS-PAGE, transferred onto a polyvinylidene difluoride membrane (Immobilon-P; Millipore, Bedford, MA), and developed with streptavidin-peroxidase (Streptavidin-HPR; Pierce) and chemiluminescence (ECL; Amersham-Pharmacia, Barcelona, Spain; Ref. 24). Western blotting with

Received 11/26/01; accepted 4/2/02.

The costs of publication of this article were defrayed in part by the payment of page charges. This article must therefore be hereby marked *advertisement* in accordance with 18 U.S.C. Section 1734 solely to indicate this fact.

<sup>1</sup> Supported by CICYT (SAF 99-0039), Gobierno de Navarra, Fundación Española de Hematología y Hemoterapia, Fundación Ramón Areces and Familia Vidal-Huarte. The Department of Immunology and Oncology at Centro Nacional de Biotecnología was founded and is supported by the Spanish Research Council (Consejo Superior de Investigaciones Científicas) and Pharmacia Corporation.

<sup>2</sup> To whom requests for reprints should be addressed, at Department of Medicine, Facultad de Medicina, Universidad de Navarra, C/Iruñlarrea, 1, 31008 Pamplona, Spain. E-mail: imelero@unav.es.

<sup>3</sup> The abbreviations used are: mAb, monoclonal antibody; Ig, immunoglobulin; LFA, leukotactic factor activity; DC, dendritic cell; DC-SIGN, dendritic cell-specific intercellular adhesion molecule-3 grabbing non-integrin; ICAM, intercellular adhesion molecule; PSD, postsource decay; MALDI, matrix-assisted desorption ionization; VEGF, vascular endothelial growth factor; bFGF, basic fibroblast growth factor; ConA, concanavalin A; FACS, fluorescence-activated cell sorter.

EOL4G8 was performed as described (25) with ascites 1/1000 or 5  $\mu$ g/ml of purified mAb in blocking solution.

**Affinity Chromatography, SDS-PAGE, and In-Gel Digestion of Proteins.** Purified EOL4G8 was covalently bound to Sepharose beads (CNBr-activated Sepharose; Amersham-Pharmacia-Biotech) according to the manufacturer's protocols. Columns were packaged in 2-ml syringes and, after conditioning with extensive washing with PBS, were loaded with PY-4.1 cell lysate from  $10^8$  cells in PBS with 1% Triton Tx-100 containing phenylmethylsulfonyl fluoride, aprotinin, and leupeptin (Sigma). Optimal elution buffer was 1 M Tris (pH 12), and 0.5-ml fractions were collected. Concentrated fractions (Centricon; Millipore, Madrid, Spain) were run in 12% SDS-PAGE, and stained protein bands were excised from the gel and then processed automatically using an Investigator ProGest protein digestion station (Genomic Solutions, Cambridgeshire, United Kingdom). Peptides were eluted with acetonitrile, 25 mM ammonium bicarbonate, and 10% formic acid (v/v) for a final extraction volume of 100  $\mu$ l.

**MALDI Peptide Mass Fingerprinting, Database Searching, and PSD MALDI Analysis.** A 0.5- $\mu$ l aliquot of the extraction solution was used to measure automatically the mass fingerprint on a Bruker Reflex III MALDI-time of flight mass spectrometer (Bruker-Franzen Analytic GmbH, Bremen, Germany) in positive ion reflector mode using delayed extraction. The measured tryptic peptide masses were transferred automatically through the MS BioTools program as inputs to search automatically the National Center for Biotechnology Information database using Mascot software (Matrix Science, London, United Kingdom). The PSD MALDI spectrum was recorded automatically, and the precursor ion was selected by FAST deflecting pulses. Data analysis was performed using Bruker BioTools 2.0 software.

**Mice and in Vivo Experimentation.** Female C57BL/6, BALB/c, and BALB/c-*nu/nu* mice (6–12-weeks old) were purchased from Jackson (Barcelona, Spain). A breeding pair of Rag2<sup>-/-</sup> mice was obtained from T. Rolink (Basel Institute for Immunology, Basel, Switzerland; Ref. 27) and bred in our animal facility. *s.c.* tumors were obtained by injection of  $5 \times 10^5$  CT26 cells into BALB/c mice,  $1 \times 10^5$  MC38 in C57BL/6 mice (18), or  $1 \times 10^6$  PY4.1 cells in BALB/c-*nu/nu* mice (19), and monitored as described (25). *s.c.* Matrigel plugs were implanted by injection of ice-cold Matrigel containing 10 ng/ml VEGF and 10 ng/ml bFGF (Peprotech, London, United Kingdom). Ten days later, plugs and surrounding tissue were paraffin-embedded and H&E stained. Endothelial cells with lumen per microscopic field ( $\times 200$ ) were counted in at least 5 fields/section and 5 sections/Matrigel plug (identity of endothelium was confirmed by immunohistochemistry with anti-Von Willibrand factor in serial sections; Refs. 25, 28, 29).

**CTL Studies and ELISAs.** Standard <sup>51</sup>Cr release were done on CT26 and P815 cells as target cells using spleen cells restimulated *in vitro* with Mytomycin-C-treated CT26 cells at a 10:1 ratio as described (25, 30).

**Adhesion Experiments.** Human monocyte-derived DCs and mouse bone marrow-derived DCs were obtained as described (18, 31). PY-4.1 cells were seeded in flat-bottomed 96-well-plates and cultured in DMEM 10% FCS until confluence was reached. Then FCS was washed, and mAbs and  $8 \times 10^4$  DCs in serum-free DMEM were added and incubated for 90 min under rotation at 60 rpm. Wells were subsequently washed five times with prewarmed DMEM, and attached DCs were counted under phase contrast microscopy in defined surfaces with a grid. Four equally placed surfaces were counted per well by an operator blinded to the experiment.

## RESULTS

**Obtainment, Selection, and Characterization of the EOL4G8 mAb.** To obtain mAbs, rats were immunized with mouse endothelial cells derived from hemangiomas raised in SV40T-transgenic mice (19, 20). A primary screening was set up to search for antibodies that could bind surface proteins on murine endothelioma cells but not on a wide panel of cell lines of epithelial origin. Thus, selected antibodies were screened for *in vivo* antitumoral effects. The antibody produced by the hybridoma EOL4G8 (rat IgG2b) fulfilled both criteria. As it can be seen in Fig. 1, *a* and *b*, EOL4G8 brightly stained the cell surface of two endothelioma cell lines that coexpressed endothelial lineage and activation markers such as CD31, CD34, the  $\alpha_v\beta_3$  integrin, ICAM-1, ICAM-2, and VCAM-1.

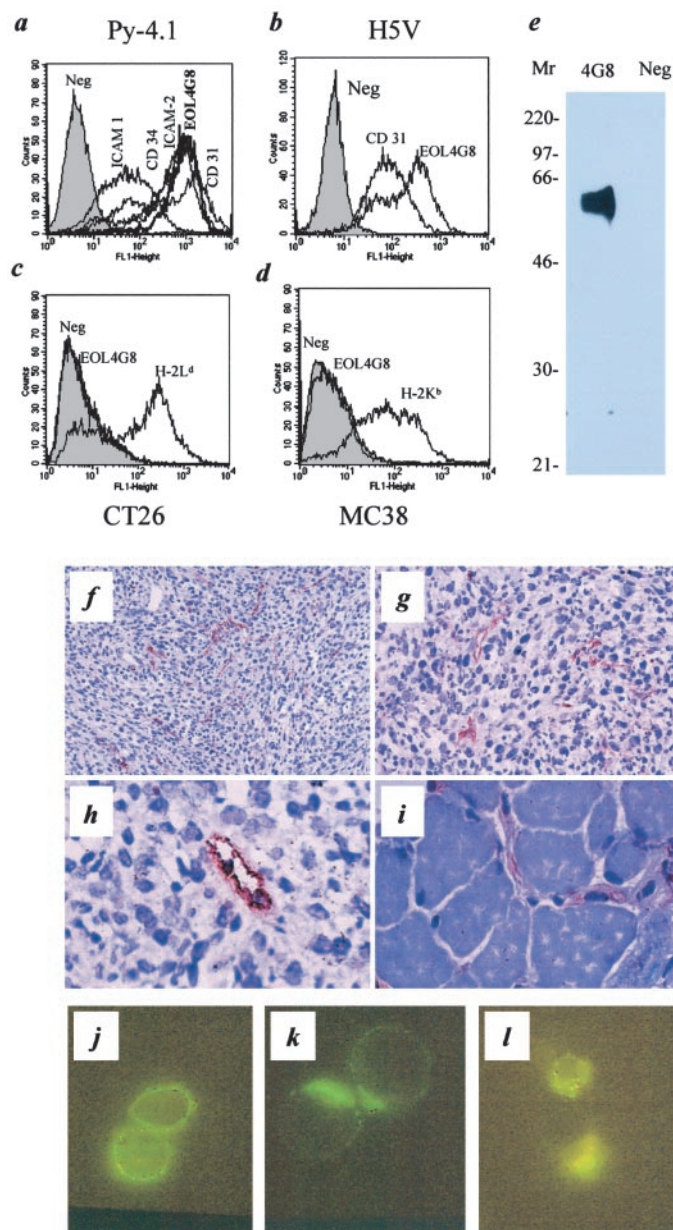


Fig. 1. EOL4G8 mAb recognizes a 59 kDa surface protein on murine endotheliomas and stains vessels in the stroma of experimental colon cancer liver metastasis. *a* and *b*, indirect immunofluorescence analyzed by FACS of the expression of the antigen recognized by EOL4G8 mAb, and the indicated surface antigens on the PY-4.1 endothelioma cell line (*a*) and the H5V endothelioma cell line (*b*). *c* and *d*, lack of detectable expression by FACS of the antigen recognized by EOL4G8 on the colon carcinoma cell lines CT26 (*c*) and MC38 (*d*). *e*, 10% SDS-PAGE analysis of immunoprecipitates obtained with EOL4G8 from lysates of PY-4.1 cells in which surface proteins had been labeled with biotin. *f*–*h*, microscopic fields at different magnifications ( $\times 100$ ,  $\times 200$ , and  $\times 400$ ) of immunohistochemical staining with EOL4G8 mAb of liver metastasis of CT26 (*i*). Representative field ( $\times 200$ ) of an immunohistochemical staining with EOL4G8 mAb of cryosections from skeletal muscle (diaphragm) from normal BALB/c mouse. *j*–*l*, indirect immunofluorescence staining of PY-4.1 with EOL4G8 mAb at 4°C (*j*) after an incubation for 25 min at 37°C (*k*) and after 1 h at 37°C (*l*). Images of UV-light microscopy are representative of at least five experiments with observation of multiple microscopic fields.

By contrast as shown in Fig. 1, *c* and *d*, EOL4G8 completely failed to detect antigens on the surface of the colon carcinoma cell lines CT26 and MC38 that were MHC class I-positive. EOL4G8 immunoprecipitated a single band of 59 kDa (Fig. 1*e*) on reducing and nonreducing conditions from lysates that had been obtained from the endothelioma cell line PY-4.1.

Immunohistochemical analysis of BALB/c livers harboring CT26-derived experimental metastasis showed a pattern of stromal staining

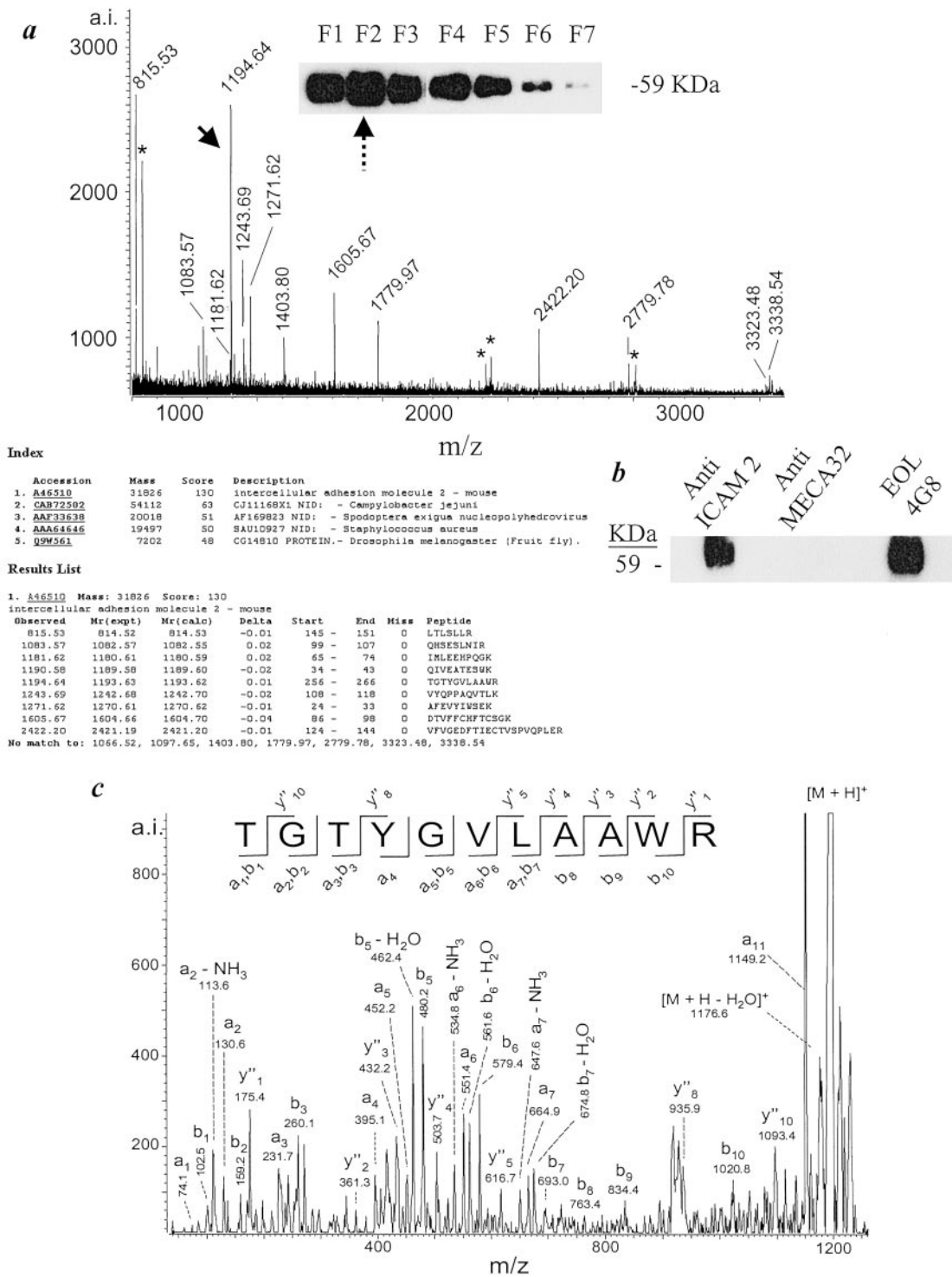


Fig. 2. EOL4G8 mAb recognizes murine ICAM-2 (CD102). *a*, MALDI fingerprinting analysis of the band in fraction 2 (visualized in the figure by Western blot with EOL4G8 mAb and marked with a dotted arrow), as it was obtained from PY-4.1 lysates using affinity chromatography columns packaged with Sepharose covalently linked to EOL4G8 mAb and analyzed subsequently by SDS-PAGE. Scores obtained on computer assisted comparison of the molecular masses of the tryptic peptides with those present in the National Center for Biotechnology Information database are summarized in the table included. *b*, 12% SDS-PAGE of immunoprecipitates obtained with commercial 3C8 anti-ICAM-2 mAb, anti MECA-32 mAb (negative control), or with EOL4G8 mAb that were developed in Western blot by EOL4G8 mAb. *c*, PSD MALDI analysis of the peak indicated by the arrow in *a*, which yields a fragment ion spectrum compatible with the sequence (detailed in the figure) proposed for that peak.

in vascular structures with lumen (Fig. 1, *f-h*). Positive cells were confirmed to be endothelial by positive immunostaining of serial sections with anti-CD31 mAb (not shown). It should be noted that the number of EOL4G8<sup>+</sup> cells in tumor stroma was outnumbered by at least 3-fold by CD31<sup>+</sup> cells, indicating that not every endothelial cell

in the malignant tissue was EOL4G8<sup>+</sup> (not shown). Interestingly, these immunohistochemical analyses did not detect any cells of healthy liver including sinusoidal and nonsinusoidal vascular structures. Positive staining with EOL4G8 mAb was also found in many vascular structures within skeletal muscle (Fig. 1*i*), whereas only a

minority of vascular structures (mainly arteriolas) were detected in brain, eye, testis, heart, and lung tissue (not shown).

On PY-4.1 cells the antigen recognized by EOL4G8 evenly decorated the plasma membrane on indirect immunofluorescence staining (Fig. 1j), but it underwent capping at 37°C for 20 min (Fig. 1k) and internalization at later time points (Fig. 1l).

Affinity chromatography with EOL4G8 mAb purified the membrane protein from PY-4.1-derived cell lysates. Elution fractions could be followed by Western blot with EOL4G8. Fraction F2 (indicated with a dotted arrow in Fig. 2a) was concentrated, run in SDS-PAGE, and the excised band was subjected to tryptic peptide fingerprinting analysis by MALDI. The database search using tryptic peptide masses observed in the MALDI peptide fingerprinting (Fig. 2a) proposed the *intercellular adhesion protein-2* from mouse as a top candidate as shown in the score table under Fig. 2a.

Furthermore, immunoprecipitates obtained with a commercial anti-mouse ICAM-2 mAb (3C8; Ref. 9) were recognized in Western blot analysis by EOL4G8 mAb depicting a band with identical electrophoretic mobility to that immunoprecipitated by EOL4G8 itself (Fig. 2b). Identification was additionally confirmed by MALDI-PSD analysis. Fig. 2c shows a recorded series of y<sup>n</sup>-, a- and b-type fragment ions generated by decomposition of the peptide at m/z = 1194.64 (peak) in the mass fingerprinting spectrum, which are compatible with its putative sequence. Molecular weight of 31.8 kDa from the predicted peptide backbone indicates heavy glycosylation if compared with the estimated 59 kDa in SDS-PAGE analysis of immunoprecipitates.

**Antitumor Effects of EOL4G8 anti-ICAM-2 mAb.** Experiments shown in Table 1 demonstrate that *in vivo* administration of EOL4G8 mAb to mice bearing established s.c. tumors derived from the injection of CT26 or MC38 cells resulted in complete regressions in an important fraction of cases. In this series of experiments the antibody was given either as ascites fluid or as purified protein. Three doses repeated every third day of 100 μl of ascites or 150 μg of purified antibody were chosen. In the first two experiments EOL4G8 was injected inside the malignant nodule in an attempt to reach high local concentrations in the tumor environment. Treatment of CT26 tumors was started on day 7 or 8 after tumor inoculation when tumor nodules rank from 4 to 7 mm (mean diameter). Injection of purified EOL4G8 mAb through i.p. route at similar doses and dosing schedule induced complete regressions in a comparable fraction of tumors, indicating

that the intratumoral route was not required. All of the tumor regressions were sustained during at least 6 months without obvious signs of tumor relapses or toxicity related to treatment.

Similar experiments were undertaken with MC38-derived tumors. In this case the effects were not curative if the onset of the i.p. regime of EOL4G8 mAb was postponed until day 7. However, two tumors of six cases completely regressed if the treatment course started on day 5. Moreover, when i.p. treatment immediately followed MC38 tumor cell inoculation, three cases of four mice underwent complete regression after transient detectable tumor growth.

Surprisingly, no antitumor activity against CT26 s.c. tumors was detected in immunodeficient BALB/c-*nu/nu* or Rag2<sup>-/-</sup> mice (in BALB/c background) suggesting a role of the immune system in the observed phenomenon.

**Mechanisms Involved in EOL4G8 Antitumor Activity.** Addressing this immune system involvement, we found that weekly depletion of CD8 cells with specific mAbs eliminated the antitumor effects of EOL4G8 (Fig. 3, a and b). Depletion of CD4 cells in a similar type of experiment did not exert a significant effect on the outcome of EOL4G8 mAb treatment (not shown). In accordance, we found in two experiments that 20 days after EOL4G8 treatment the spleen of mice bearing CT26 s.c. tumors had specific antitumor CTL activity (Fig. 3c) that was not detected in mice treated with control antibody. Furthermore, tumors 7 days after treatment showed a prominent infiltrate of mononuclear cells (especially around vessels) also with some granulocytes, including eosinophils and areas of tumor necrosis (Fig. 3d).

Resting murine T lymphocytes expressed barely detectable levels of ICAM-2 but concanavalin + interleukin 2 stimulated T lymphoblasts readily expressed this molecule with high intensity (Fig. 3e, f). Therefore, a potential way of action of the antibody was to provide costimulatory signals to activated ICAM-2<sup>+</sup> antitumor T cells. Nonetheless we could not demonstrate any activity of EOL4G8 mAb to provide costimulation to suboptimal stimulation with anti-CD3 antibodies *in vitro* either to induce proliferation or IFN-γ secretion, regardless of the extensive series of experimental conditions under which anti-CD28 used as a positive control readily costimulated these effects (not shown). Those conditions included rested T-cell blasts that intensely expressed ICAM-2 and mixed lymphocyte culture-type cultures of T cells and fully allogeneic DCs. In both cases EOL4G8 mAb, either attached to plastic or in soluble form, failed to modify the response to suboptimal anti-CD3 mAb or alloantigens.

We carried out experiments to assess a potential antiangiogenic effect of this antibody although the antitumor activity could not be explained solely by antiangiogenesis because it was not found in immunodeficient mice. The subject was studied by implanting Matrigel plugs embedded in VEGF + bFGF in nude mice and assessing the number of endothelial cells in microscopic fields within the Matrigel plug. An inhibition (≈ 30%) induced by EOL4G8 mAb was found in comparison with mice treated with control antibodies (Fig. 3g). Furthermore, EOL4G8 was able to decrease the rate of progression of PY-4.1-derived hemangiomas in nude mice indicating the ability of the antibody to interfere *in vivo* with the growth of these ICAM-2<sup>+</sup>-transformed endothelial cells (Fig. 3h).

**EOL4G8 mAb Provokes Attachment of DCs to ICAM-2<sup>+</sup> Endothelial Cells.** Incubation of PY-4.1 cells *in vitro* with EOL4G8 did not result in changes in cell viability, morphology, proliferation, or tubulization on Matrigel. However, we found that preincubation of a monolayer of PY-4.1 with EOL4G8 induced the adhesion to it of a DC line (D2SC/1) that represents DCs at an immature status (Ref. 21; Fig. 4a). This effect was not observed with control antibodies including a commercially available antimurine ICAM-2 antibody (3C8). The increased adhesion was not blocked by an anti-LFA-1 mAb that inhibits

Table 1 Antitumor effects of treatment of established s.c. tumors with EOL-4G8 mAb<sup>a</sup>

Tumor/strain	Route/days	mAb form	Treatment		
			Saline	EOL4G8	IgG
CT26/BALB/c	i.t. <sup>b</sup> 7, 10, 12	Ascites <sup>c</sup>	0/4	3/4	ND
	i.t. 8, 10, 13	purificate <sup>d</sup>	0/4	4/4	1/4
	i.p. 8, 10, 12	purificate	0/3	5/6	0/4
MC38/C57BL/6	i.p. 7, 10, 12	purificate	ND	4/6	0/6
	i.p. 0, 3, 7, 10	purificate	0/4	3/4	0/4
	i.p. 5, 8, 11	purificate	0/6	2/6	0/7
CT26 BALB/c- <i>nu/nu</i>	i.t. 7, 9, 11, 18	purificate	0/5	0/5	0/5
	i.p. 0, 3, 7, 10	Ascites	0/2	0/4	ND
	i.p. 5, 8, 11	purificate	0/4	0/4	ND
CT26 BALB/c Rag 2 <sup>-/-</sup>	i.p. 0, 3, 7, 10	purificate	0/6	0/6	ND

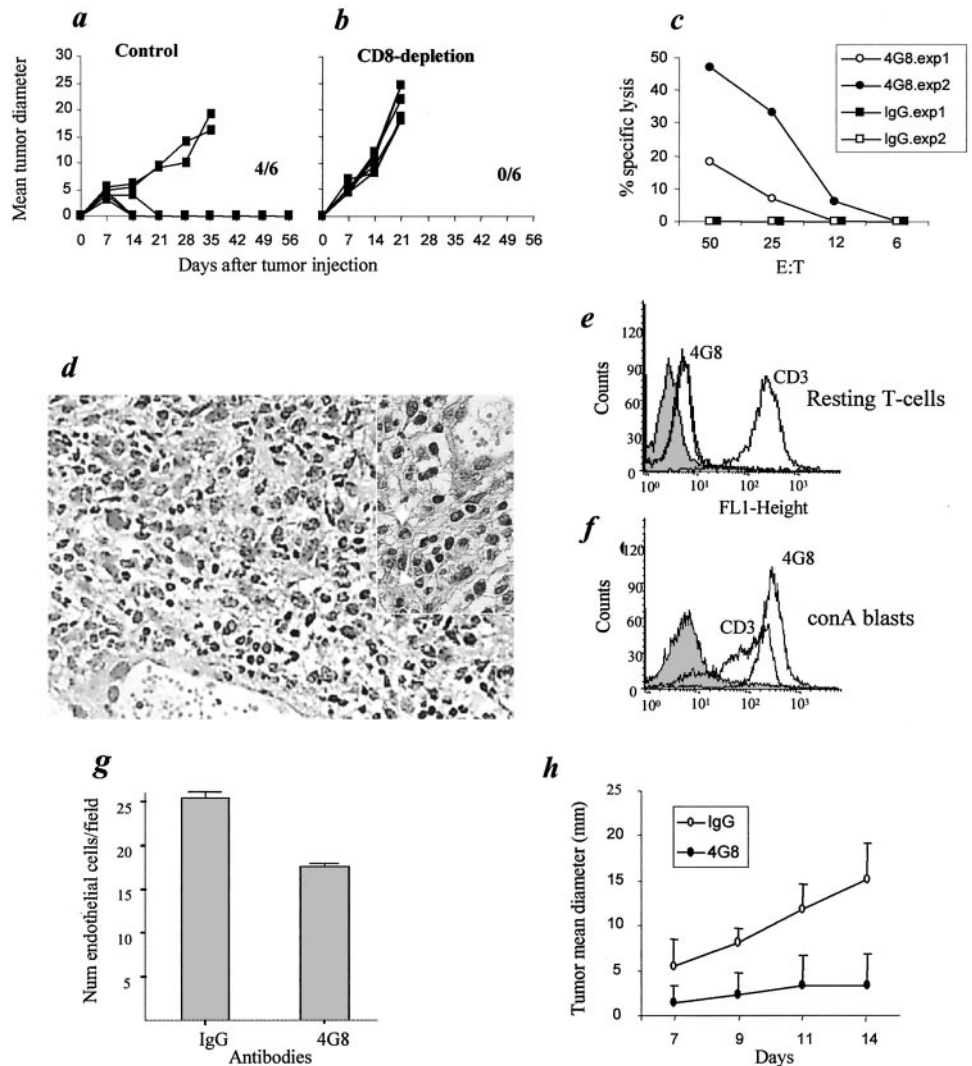
<sup>a</sup> Fraction of tumor-free surviving mice (number of cured mice/total number of mice) in different experiments 24 weeks after being injected s.c. in the right flank with the indicated tumor cell lines to develop tumor nodules. Mice were treated with the indicated antibody doses, via the indicated routes, on the indicated days after tumor inoculation. In some cases mice received an equivalent volume of saline buffer or polyclonal rat IgG as a control. Mice were terminated when tumor nodules surpassed 24 mm (mean diameter) or were followed up for 6 months if disease-free.

<sup>b</sup> i.t., intratumoral; i.p., intraperitoneal; ND, not done.

<sup>c</sup> Ascites fluid drained from peritoneal cavity of athymic nude mice injected i.p. with the EOL4G8 hybridoma; 100 μl were given per dose.

<sup>d</sup> Purified antibody obtained with protein G Sepharose columns from ascites fluid that was given at 150 μg/dose.

Fig. 3. Treatment with EOL4G8 mAb stimulates antitumor CTL-mediated immune responses and can interfere with endothelial cells *in vivo*. *a*, follow-up of tumor mean diameters of CT26 tumors in mice receiving 150  $\mu$ g i.p. of EOL 4G8 mAb on days 7, 10, and 12 after tumor inoculation. *b*, similar to *a*, but in this case mice received 100  $\mu$ l of ascites containing depleting anti-CD8 mAb on days 6, 14, and 21 after tumor inoculation. *c*, CTL activity against CT26 in 4-hour <sup>51</sup>Cr release assays of splenocytes obtained from mice bearing s.c. CT26 tumors treated on days 7, 10, and 12 with 150  $\mu$ g of EOL4G8 or control rat IgG. Results from two independent experiments with two mice/group are shown. Specificity was checked by lack of cytotoxicity of P815 cells in experiments performed in parallel (not shown). *d*, H&E staining of sections obtained from a representative s.c. CT26 tumor taken 14 days after tumor cell inoculation once mice had received treatment with two doses of 150  $\mu$ g of EOL4G8 mAb given on days 6 and 8. A ( $\times 100$ ) magnification field is shown with a detail ( $\times 200$ ) shown in the top right corner of the picture. Eosinophils are indicated by the arrows. *e* and *f*, expression of ICAM-2 as detected by EOL4G8 and FACS analysis in magnetic bead-purified T cells from normal resting BALB/c spleens containing 29% CD8<sup>+</sup> cells and 60% CD4<sup>+</sup> cells (*e*) and in those lymphocytes after activation with 2  $\mu$ g/ml of ConA plus 500 IU of human recombinant interleukin 2 for 4 days (*f*). Results were confirmed with the 3C8 anti ICAM-2 mAb (not shown). *g*, vascularization of Matrigel implants embedded in VEGF and bFGF placed under the skin of BALB/c nude mice that received 150  $\mu$ g of EOL4G8 or control antibody on days 0 and 3 after Matrigel injection, measured as the number of endothelial cells in microscopic fields ( $\times 200$ ) from H&E-stained sections. Four Matrigel plugs were implanted in each mouse with a total of seven mice/group, and data were from five sections from each plug. Statistical significance was  $P < 0.01$  according to Student's *t* test. *h*, sequential hemangioma growth (assessed by mean diameter in mm) under the skin of BALB/c nude mice injected with 10<sup>6</sup> PY-4.1 cells on day 0 and treated with EOL4G8 mAb or control rat IgG (150  $\mu$ g/i.p. dose) on days 3, 6, and 9; bars,  $\pm$ SD.



its binding to ICAM-1 and remained unaffected by an antibody that also binds a surface molecule of endothelial cells (anti-MECA-32). The augment of cell adhesion took place at 4°C and when soluble nonattached mAb had been removed indicating that this phenomenon did not require active metabolism nor direct access of soluble antibody to the DC line (Fig. 4*a*). Furthermore, EOL4G8 mAb was able to promote adhesion of DCs to affinity-purified PY-4.1-derived ICAM-2, showing that enhancement of adhesion took place irrespective on whether ICAM-2 was or was not attached to a cell surface (Fig. 4*b*). D2SC/1 also expresses low levels of ICAM-2 and, therefore, EOL4G8 could be acting on the DC side. (Fig. 4*c*). EOL4G8-increased adhesion is dependent on divalent cations because it is inhibited by EGTA (Fig. 4*d*) and is dependent on the tubulin cytoskeleton of DCs as deduced from inhibitions observed with colchicine (Fig. 4*d*). Enhancement of adhesion by EOL4G8 also took place with cultured bone marrow-derived murine DCs thus excluding artifacts because of the transformed phenotype of the D2SC/1 cell line (Fig. 4*e*).

**EOL4G8 mAb Enhances Adhesion of Human DCs to Mouse Endothelium in a DC-SIGN-mediated Fashion.** EOL4G8 also increases the adhesion of human DCs to the murine endothelioma PY-4.1 (Fig. 5*a*), although the antibody does not bind human ICAM-2 nor does it stain human DCs (FACS histogram in Fig. 5*a*). Therefore, the antibody in this case cannot bind both cell surfaces to form a

bridge between them. Instead the mechanism seems to be that EOL4G8 binding modifies ICAM-2 in such a way that it becomes more prone to interact with a putative ligand on human DCs that are not LFA-1, as deduced from the lack of inhibition observed with an anti-CD18 mAb that blocks LFA-1-dependent adhesion (Fig. 5*b*). As shown in Fig. 5*b*, an anti-DC-SIGN mAb (MR-1) (23) inhibits 40–50% of the EOL4G8-induced adhesion of human DCs to mouse PY-4.1 endothelioma cells. To additionally confirm the involvement of DC-SIGN, a series of experiments was carried out with transfectants in human K562 cells, which stably expressed DC-SIGN (FACS histogram under Figs. 5, *c* and *d*) or in equivalent untransfected cells. As it can be seen in Fig. 5*c*, EOL4G8 mAb intensely promoted the adhesion of the DC-SIGN<sup>+</sup> transfectant to PY-4.1 cells, whereas it did not modify the adhesion of the untransfected K562 cells (Fig. 5*d*). Moreover the mAb against DC-SIGN inhibited >60% of the adhesion of DC-SIGN<sup>+</sup> K562 to mouse endothelium. All of these results strongly indicate that EOL4G8 enhances tumor immunity by promoting the adhesion of ICAM-2<sup>+</sup> cells to DC-SIGN molecules expressed on DCs.

## DISCUSSION

This study shows that *in vivo* injection of a mAb that recognizes ICAM-2 (CD102) eradicates experimental solid tumors that do not

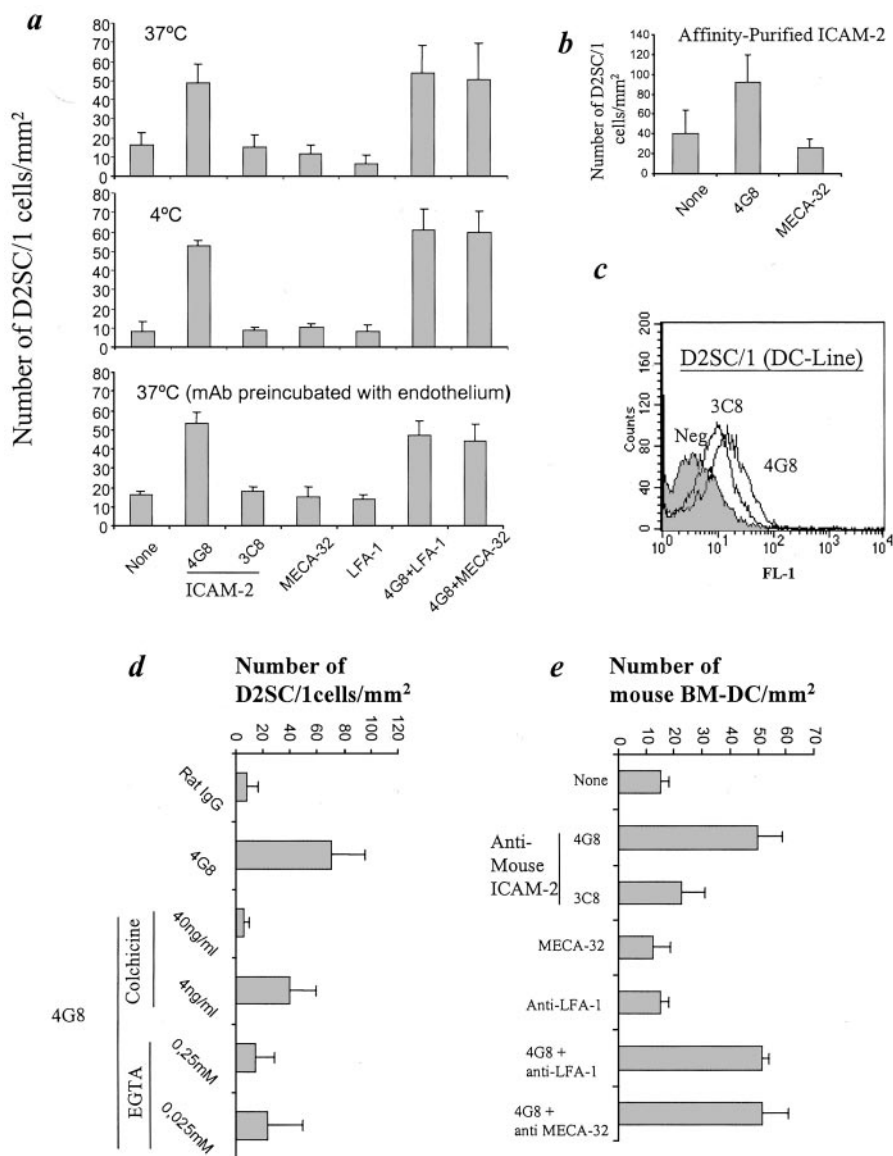


Fig. 4. EOL4G8 enhances the adhesion of DCs to mouse endothelial cells expressing ICAM-2. *a*, adhesion of D2SC/1 dendritic immortalized cell line to confluent monolayers of PY-4.1 cells assessed by counting DC cells/mm<sup>2</sup> under phase contrast microscopy after washing unbound cells. Results are mean of four counts of equally placed fields inside triplicate wells. Indicated antibodies were used at a concentration 5  $\mu$ g/ml and added during the assay (*top panels*) or preincubated during 1 h at 4°C and then washed three times before addition of D2SC/1 cells (*bottom panel*); *b*) Adhesion to PY-4.1 cells assessed as in *a* to wells coated with 2  $\mu$ g/ml of purified ICAM-2 protein from fraction 3 (F3) in Fig. 2*a*. *c*, FACS analysis of the expression of ICAM-2 on D2SC/1 cells (isotype matched negative control in a shaded histogram); *d*, adhesion experiments as in *a* but in which the indicated concentrations of colchicine or EGTA were included during the assays. *e*, adhesion experiments to monolayers of PY4.1 cells performed similarly to those in *a* and *d* but in which mouse bone marrow-derived DCs were used instead of D2SC/1 cells; bars,  $\pm$ SD.

express ICAM-2. Hence, the antibody required the contribution of endogenous mechanisms to interfere with cancer progression. Ineffectiveness of the antibody in nude and rag2<sup>-/-</sup> mice pointed out an absolute requirement of T cells. Depletion experiments with anti-CD8 mAb clearly showed that CTLs were required for antitumor effects, and this fact correlated with the detection of antitumor-specific CTL activity in EOL4G8-treated mice. mAbs that enhance the antitumor immune response to produce therapeutic immunity have been described. The most potent seem to be anti-CTLA-4 (2), anti-4-1BB (3), and anti-CD40 (4). Each of them acts through different mechanisms that share the activation of a CTL response against the tumor as the final effector mechanism.

ICAM-2 is readily expressed on murine activated T cells but very poorly so on resting T cells. Thus, it was conceivable that EOL4G8 could be providing costimulatory signals to T cells pre-activated through the T-cell receptor. However all of our attempts to show that costimulatory activity for proliferation or cytokine secretion *in vitro* have failed. Therefore, it is still unresolved whether ICAM-2 artificial ligation with EOL4G8 mAb on T cells would be involved in the observed antitumor effects by direct signals through ICAM-2. ICAM-2 bound by mAbs has not been

involved yet in active signaling unlike the case of related molecules such as ICAM-1 (32), ICAM-3 (33), and VCAM-1 (34). The reported intracytoplasmic interactions of ICAM-2 with cytoskeletal proteins (35, 36) may be involved in these phenomena, and are consistent with our observations on the capping and internalization induced by EOL4G8.

CTL activity and the lymphoid infiltration of tumors after systemic treatment with EOL4G8 speak of an activation of the immune system provoked by the antibody *in vivo*. The presence of granulocytes in the infiltrate is also interesting and resembles to some extent observations in tumors transfected to produce certain cytokines (37) or fas-L (38, 39). Because CT26 is more immunogenic than MC38 (18), the higher efficacy of EOL4G8 treatment on CT26-derived tumors indicates that EOL4G8 amplifies a weak, preexisting immune response. The basal immunogenicity of CT26 cells is best indicated by experiments that show a slower growth of these transplanted tumors in BALB/c mice than in Rag-2<sup>-/-</sup> syngeneic mice.<sup>4</sup>

<sup>4</sup> I. Tirapu *et al.* submitted for publication.

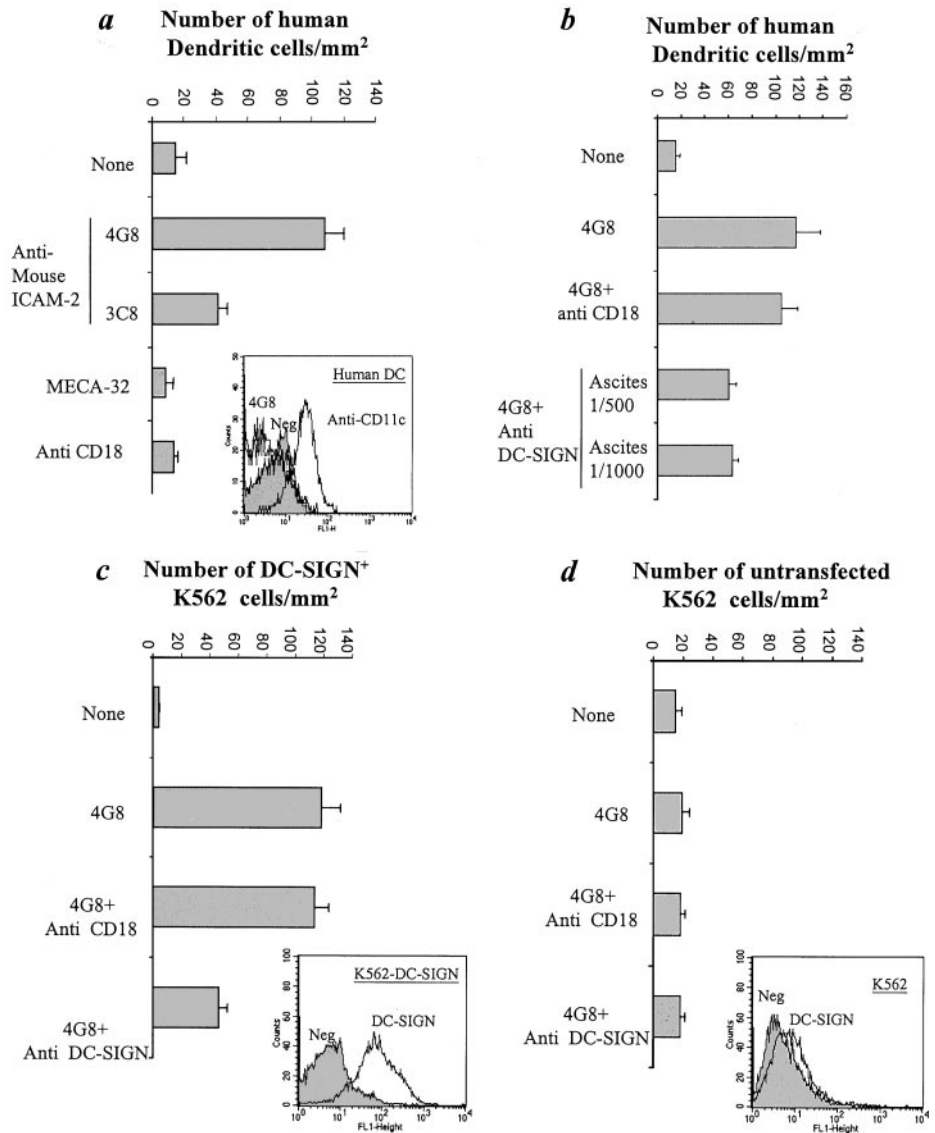


Fig. 5. EOL4G8 augments the adhesion of human DCs and of a human transfected cell line expressing DC-SIGN to mouse endothelium. *a*, adhesion experiments to monolayers of PY-4.1 murine endothelial cell line similarly performed to those in Fig. 4 but in which human monocyte-derived DCs were used instead of DCs of murine origin. Lack of staining of these human DCs with the antimurine ICAM-2 mAbs EOL4G8 and 3C8 is shown in the FACS histogram within the panel. *b*, inhibition of EOL4G8 induced adhesion of human DCs to PY4.1 cells as detected on incubation with the indicated mAbs. *c*, adhesion of K562 cells transfected to stably express DC-SIGN onto a confluent monolayer of PY-4.1 cells in the presence of the indicated antibodies. *d*, adhesion experiments identically performed as in *c* but with untransfected control K562 cells. FACS analysis of the levels of expression of DC-SIGN on staining with a specific mAb (MR-1) are shown within *c* and *d*; bars,  $\pm$ SD.

Carbohydrates attached to ICAM-2 are ligands of the DC-SIGN lectin (10). DC-SIGN on interaction with ICAM-3 has been found instrumental for the early low avidity interactions of DCs and T cells (12). Our results show an enhanced attachment of immature DCs to endothelial cells on incubation with EOL4G8. Because EOL4G8 stains with some degree of selectivity tumor endothelium, it is possible that the mAb favors recruitment of DCs into malignant tissue. Besides it is tempting to speculate that the antibody would modify ICAM-2/DC-SIGN interactions at the immunological synapse between lymphocytes and DCs. Our data with the interspecies adhesion systems, involving human DCs and mouse endothelial cells, strongly suggest that EOL4G8 operates increasing the adhesion of ICAM-2 to DC-SIGN. The involvement of human DC-SIGN is shown both by antibody blocking and by transmission of the activity on transfection of the DC-SIGN-encoding cDNA. Definitive proof of such hypotheses awaits additional characterization on the function of mouse homologues of DC-SIGN (16).

EOL4G8 binds ICAM-2 at an epitope that interferes with LFA-1 binding (an activity that maps to the NH<sub>2</sub>-terminal Ig domain of ICAM-2; Refs. 7, 8, 13) but which could up-regulate somehow the binding to DC-SIGN (an activity dependent on the COOH-terminal Ig domain of human ICAM-2 and its attached carbohydrates; Ref. 13).

Peculiar functional properties of the epitope bound by EOL4G8 mAb might be crucial to understand its biological properties. This is supported by our observation that another antibody against ICAM-2 (3C8), which also interferes with adhesion to LFA-1 (Ref. 9; although it binds to a noncompeting epitope), fails to up-regulate DC adhesion to endothelium. A conformational change induced by EOL4G8 in the protein backbone of ICAM-2 or its attached carbohydrates, enhancing its adhesiveness to DC-SIGN, could be the intimate mechanism of action. This is our best-fitting explanation to the observation that EOL4G8 also enhances binding of DCs to immunopurified ICAM-2 attached to plastic. We cannot exclude that other putative ICAM-2-binding lectins might also be involved.

EOL4G8 inhibits angiogenesis of Matrigel implants, but such an effect, although detectable, was very weak in comparison to inhibitions reported for other agents of which the efficacy is entirely dependent on this mechanism (28, 29, 40). An appraisal of the real extent of the contribution of antiangiogenesis to the overall EOL4G8 efficacy is difficult, but this mechanism is not sufficient to cause macroscopic antitumor activity in immunodeficient mice.

As a whole our studies define ICAM-2 as a new target for antibodies mediating antitumor effects through indirect mechanisms that seem to include enhancement of the intrinsic adhesion properties of



this molecule. *In vivo*, the injected antibody finds its cognate antigen mainly on activated T cells and on endothelial cells, and is subsequently capable to ignite antitumor immune mechanisms that can eradicate established tumors.

## ACKNOWLEDGMENTS

We thank Drs. Francisco Sánchez-Madrid, Lieping Chen, Juan José Lasarte, Gloria González, Cheng Qian, Maurizio Bendandi, and Puri Fortes for helpful suggestions and critical reading. We also thank Drs. V. Bautch, A. Mantovani, and P. Ricciardi-Castagnoli for their generous gifts of cell lines. Excellent animal facility assistance by Juan Percz and Javier Guillén is also acknowledged.

## REFERENCES

- Green, M. C., Murray, J. L., and Hortobagyi, G. N. Monoclonal antibody therapy for solid tumors. *Cancer Treat. Rev.*, 26: 269–286, 2000.
- Leach, D. R., Krummel, M. F., and Allison, J. P. Enhancement of antitumor immunity by CTLA-4 blockade. *Science (Wash. DC)*, 271: 1734–1736, 1996.
- Melero, I., Shuford, W. W., Newby, S. A., Aruffo, A., Ledbetter, J. A., Hellstrom, K. E., Mittler, R. S., and Chen, L. Monoclonal antibodies against the 4–1BB T-cell activation molecule eradicate established tumors. *Nat. Med.*, 3: 682–685, 1997.
- French, R. R., Chan, H. T., Tutt, A. L., and Glennie, M. J. CD40 antibody evokes a cytotoxic T-cell response that eradicates lymphoma and bypasses T-cell help. *Nat. Med.*, 5: 548–553, 1999.
- Brooks, P. C., Stromblad, S., Klemke, R., Visscher, D., Sarkar, F. H., and Cheresh, D. A. Anti-integrin  $\alpha v \beta 3$  blocks human breast cancer growth and angiogenesis in human skin. *J. Clin. Invest.*, 96: 1815–1822, 1995.
- Schlaeppli, J. M., and Wood, J. M. Targeting vascular endothelial growth factor (VEGF) for anti-tumor therapy, by anti-VEGF neutralizing monoclonal antibodies or by VEGF receptor tyrosine-kinase inhibitors. *Cancer Metastasis Rev.*, 18: 473–481, 1999.
- de Fougerolles, A. R., Stacker, S. A., Schwarting, R., and Springer, T. A. Characterization of ICAM-2 and evidence for a third counter-receptor for LFA-1. *J. Exp. Med.*, 174: 253–267, 1991.
- Staunton, D. E., Dustin, M. L., and Springer, T. A. Functional cloning of ICAM-2, a cell adhesion ligand for LFA-1 homologous to ICAM-1. *Nature (Lond.)*, 339: 61–64, 1989.
- Xu, H., Bickford, J. K., Luther, E., Carpenito, C., Takei, F., and Springer, T. A. Characterization of murine intercellular adhesion molecule-2. *J. Immunol.*, 156: 4909–4914, 1996.
- Geijtenbeek, T. B., Krooshoop, D. J., Bleijs, D. A., van Vliet, S. J., van Duijnhoven, G. C., Grabovsky, V., Alon, R., Figdor, C. G., and van Kooyk, Y. DC-SIGN-ICAM-2 interaction mediates dendritic cell trafficking. *Nat. Immunol.*, 1: 353–357, 2000.
- Geijtenbeek, T. B., Kwon, D. S., Torensma, R., van Vliet, S. J., van Duijnhoven, G. C., Middel, J., Cornelissen, I. L., Nottet, H. S., KewalRamani, V. N., Littman, D. R., Figdor, C. G., and van Kooyk, Y. DC-SIGN, a dendritic cell-specific HIV-1-binding protein that enhances *trans*-infection of T cells. *Cell*, 100: 587–597, 2000.
- Geijtenbeek, T. B., Torensma, R., van Vliet, S. J., van Duijnhoven, G. C., Adema, G. J., van Kooyk, Y., and Figdor, C. G. Identification of DC-SIGN, a novel dendritic cell-specific ICAM-3 receptor that supports primary immune responses. *Cell*, 100: 575–585, 2000.
- Bleijs, D. A., Geijtenbeek, T. B., Figdor, C. G., and van Kooyk, Y. DC-SIGN and LFA-1: a battle for a ligand. *Trends Immunol.*, 22: 457–463, 2001.
- Mitchell, D. A., Fadden, A. J., and Drickamer, K. A novel mechanism of carbohydrate recognition by the C-type lectins DC-SIGN and DC-SIGNR: Subunit organization and binding to multivalent ligands. *J. Biol. Chem.*, 276: 30, 2001.
- Bromley, S. K., Burack, W. R., Johnson, K. G., Somersalo, K., Sims, T. N., Sumen, C., Davis, M. M., Shaw, A. S., Allen, P. M., and Dustin, M. L. The immunological synapse. *Annu. Rev. Immunol.*, 19: 375–396, 2001.
- Park, C. G., Takahara, K., Umemoto, E., Yashima, Y., Matsubara, K., Matsuda, Y., Clausen, B. E., Inaba, K., and Steinman, R. M. Five mouse homologues of the human dendritic cell C-type lectin, DC-SIGN. *Int. Immunol.*, 13: 1283–1290, 2001.
- Gerwin, N., Gonzalo, J. A., Lloyd, C., Coyle, A. J., Reiss, Y., Banu, N., Wang, B., Xu, H., Avraham, H., Engelhardt, B., Springer, T. A., and Gutierrez-Ramos, J. C. Prolonged eosinophil accumulation in allergic lung interstitium of ICAM-2 deficient mice results in extended hyperresponsiveness. *Immunity*, 10: 9–19, 1999.
- Melero, I., Duarte, M., Ruiz, J., Sangro, B., Galofre, J., Mazzolini, G., Bustos, M., Qian, C., and Prieto, J. Intratumoral injection of bone-marrow derived dendritic cells engineered to produce interleukin-12 induces complete regression of established murine transplantable colon adenocarcinomas. *Gene Ther.*, 6: 1779–1784, 1999.
- Dubois, N. A., Kolpack, L. C., Wang, R., Azizkhan, R. G., and Bautch, V. L. Isolation and characterization of an established endothelial cell line from transgenic mouse hemangiomas. *Exp. Cell Res.*, 196: 302–313, 1991.
- Bussolino, F., De Rossi, M., Sica, A., Colotta, F., Wang, J. M., Bocchietto, E., Padura, I. M., Bosisio, A., Dejana, E., and Mantovani, A. Murine endothelioma cell lines transformed by polyoma middle T oncogene as target for and producers of cytokines. *J. Immunol.*, 147: 2122–2129, 1991.
- Paglia, P., Girolomoni, G., Robbiati, F., Granucci, F., and Ricciardi-Castagnoli, P. Immortalized dendritic cell line fully competent in antigen presentation initiates primary T cell responses *in vivo*. *J. Exp. Med.*, 178: 1893–1901, 1993.
- Paglia, P., Chiodoni, C., Rodolfo, M., and Colombo, M. P. Murine dendritic cells loaded *in vitro* with soluble protein prime cytotoxic T lymphocytes against tumor antigen *in vivo*. *J. Exp. Med.*, 183: 317–322, 1996.
- Relloso, M., Puig-Kroger, A., Pello, O. M., Rodriguez-Fernandez, J. L., de la Rosa, G., Longo, N., Navarro, J., Muñoz Fernandez, M. A., Sanchez-Mateos, P., and Corbí, A. L. DC-SIGN (CD209) expression is IL-4 dependent and is negatively regulated by IFN, TGF $\beta$  and anti-inflammatory agents. *J. Immunol.*, 168: 2634–2643, 2002.
- Rodriguez-Calvillo, M., Gabari, I., Duarte, M., Mazzolini, G., Rifon, J., Rocha, E., Prieto, J., and Melero, I. Thrombopenic purpura induced by a monoclonal antibody directed to a 35-kilodalton surface protein (p35) expressed on murine platelets and endothelial cells. *Exp. Hematol.*, 29: 589–595, 2001.
- Narvaiza, I., Mazzolini, G., Barajas, M., Duarte, M., Zaratiegui, M., Qian, C., Melero, I., and Prieto, J. Intratumoral coinjection of two adenoviruses, one encoding the chemokine IFN-gamma-inducible protein-10 and another encoding IL-12, results in marked antitumoral synergy. *J. Immunol.*, 164: 3112–3122, 2000.
- Melero, I., Balboa, M. A., Alonso, J. L., Yague, E., Pivel, J. P., Sanchez-Madrid, F., and Lopez-Botet, M. Signaling through the LFA-1 leucocyte integrin actively regulates intercellular adhesion and tumor necrosis factor- $\alpha$  production in natural killer cells. *Eur. J. Immunol.*, 23: 1859–1865, 1993.
- Rolink, A., Melchers, F., and Andersson, J. The SCID but not the RAG-2 gene product is required for S  $\mu$ -S epsilon heavy chain class switching. *Immunity*, 5: 319–330, 1996.
- Angiolillo, A. L., Sgadari, C., Taub, D. D., Liao, F., Farber, J. M., Maheshwari, S., Kleinman, H. K., Reaman, G. H., and Tosato, G. Human interferon-inducible protein 10 is a potent inhibitor of angiogenesis *in vivo*. *J. Exp. Med.*, 182: 155–162, 1995.
- Barajas, M., Mazzolini, G., Genove, G., Bilbao, R., Narvaiza, I., Schmitz, V., Sangro, B., Melero, I., Qian, C., and Prieto, J. Gene therapy of orthotopic hepatocellular carcinoma in rats using adenovirus coding for interleukin 12. *Hepatology*, 33: 52–61, 2001.
- Mazzolini, G., Qian, C., Narvaiza, I., Barajas, M., Borrás-Cuesta, F., Xie, X., Duarte, M., Melero, I., and Prieto, J. Adenoviral gene transfer of interleukin 12 into tumors synergizes with adoptive T cell therapy both at the induction and effector level. *Hum. Gene Ther.*, 11: 113–125, 2000.
- Sallusto, F., and Lanzavecchia, A. Efficient presentation of soluble antigen by cultured human dendritic cells is maintained by granulocyte/macrophage colony-stimulating factor plus interleukin 4 and downregulated by tumor necrosis factor  $\alpha$ . *J. Exp. Med.*, 179: 1109–1118, 1994.
- Koyama, Y., Tanaka, Y., Saito, K., Abe, M., Nakatsuka, K., Morimoto, I., Auron, P. E., and Eto, S. Cross-linking of intercellular adhesion molecule 1 (CD54) induces AP-1 activation and IL-1 $\beta$  transcription. *J. Immunol.*, 157: 5097–5103, 1996.
- Cid, M. C., Esparza, J., Juan, M., Miralles, A., Ordi, J., Vilella, R., Urbano-Marquez, A., Gaya, A., Vives, J., and Yague, J. Signaling through CD50 (ICAM-3) stimulates T lymphocyte binding to human umbilical vein endothelial cells and extracellular matrix proteins via an increase in  $\beta 1$  and  $\beta 2$  integrin function. *Eur. J. Immunol.*, 24: 1377–1382, 1994.
- Lazaar, A. L., Krymskaya, V. P., and Das, S. K. VCAM-1 activates phosphatidylinositol 3-kinase and induces p120Cbl phosphorylation in human airway smooth muscle cells. *J. Immunol.*, 166: 155–161, 2001.
- Heiska, L., Alftan, K., Gronholm, M., Vilja, P., Vaheri, A., and Carpen, O. Association of ezrin with intercellular adhesion molecule-1 and -2 (ICAM-1 and ICAM-2). Regulation by phosphatidylinositol 4, 5-bisphosphate. *J. Biol. Chem.*, 273: 21893–21900, 1998.
- Yonemura, S., Hirao, M., Doi, Y., Takahashi, N., Kondo, T., and Tsukita, S. Ezrin/radixin/moesin (ERM) proteins bind to a positively charged amino acid cluster in the juxta-membrane cytoplasmic domain of CD44, CD43, and ICAM-2. *J. Cell Biol.*, 140: 885–895, 1998.
- Tepper, R. I., Coffman, R. L., and Leder, P. An eosinophil-dependent mechanism for the antitumor effect of interleukin-4. *Science (Wash. DC)*, 257: 548–551, 1992.
- Seino, K., Kayagaki, N., Okumura, K., and Yagita, H. Antitumor effect of locally produced CD95 ligand. *Nat. Med.*, 3: 165–170, 1997.
- Drozdzik, M., Qian, C., Lasarte, J. J., Bilbao, R., and Prieto, J. Antitumor effect of allogenic fibroblasts engineered to express Fas ligand (FasL). *Gene Ther.*, 5: 1622–1630, 1998.
- Boehm, T., Folkman, J., Browder, T., and O'Reilly, M. S. Antiangiogenic therapy of experimental cancer does not induce acquired drug resistance. *Nature (Lond.)*, 390: 404–407, 1997.